FIR SMOOTHING OF DISCRETE-TIME STATE-SPACE MODELS WITH APPLICATIONS TO CLOCKS

Oscar Ibarra-Manzano, Luis Morales-Mendoza, Yuriy S. Shmaliy

Electronics Department, Guanajuato University
Ctra. Salamanca-Valle, 3.5+1.8km, Palo-Blanco, 36855, Salamanca, Mexico
phone: + 52 (464) 647-01-95, email: shmaliy@ugto.mx,
web: www.ingenierias.ugto.mx

ABSTRACT

We address a smoothing finite impulse response (FIR) filter for discrete time-invariant state-space polynomial models commonly used to model signals over finite data. A general gain is derived for the relevant p-lag unbiased smoothing FIR filter. An application is given for the time interval errors of local slave clocks of digital communications networks. An excellent performance of the best unbiased fit is demonstrated along with its ability to extrapolate linearly the clock behaviors for holdover required by the IEEE Standards.

1. INTRODUCTION

Estimation and denoising of polynomial models measured in different noise environment is efficiently provided using the finite impulse response (FIR) p-lag smoothers [1–3], relating the estimate to the past discrete point $n+p$, $p<0$, or smoothing FIR filters [4, 5], which estimates are provided at the present point n via past and future. In digital networks employing local time scales formed by precision local clocks [6, 7], smoothing commonly solves three main problems. It can be used to estimate the initial clock state for the Kalman filtering of clock state, provide maximum denoising at some past points [1, 4], and obtain the best fit in order to predict future clock behaviors [8, 9]. The latter is especially important for "holdover", when a synchronizing signal is temporary not available [10].

Because noise in clocks is not white [6], the best fit is achieved if one uses an averaging FIR smoother structure [11, 12] and not the recursive Kalman one. Although some recent efforts were made in this direction for clocks [13, 14], a general p-lag smoothing FIR filter for discrete-time state-space polynomial models still was not addressed. In this paper, we solve this problem in general terms for a variety of applications and give an examples for a slave precision crystal clock of a digital communications network node and a master clock.

2. POLYNOMIAL SIGNAL MODEL

Consider a signal x_{kn} representing the kth state, $k\in[1,K]$, of a K-state system. Suppose that a polynomial signal x_{1n}, $k=1$, representing the first state is projected from $n-N+1-p$ to n with the finite Taylor series expansion of order $K-1$ and a lag $p<0$ as follows [15]:

$$x_{1n}=\sum_{q=0}^{K-1}x_{(q+1)(n-N+1-p)}\frac{\tau^q(N-1+p)^q}{q!}\,, \tag{1}$$

where $x_{(q+1)(n-N+1-p)}$, $q\in[0,K-1]$, is the $(q+1)$-state at $n-N+1-p$ and the signal thus characterized with K states, from 1 to K. Here, τ is the sampling time. Also suppose that a signal x_{kn} is coupled with $x_{(k-1)n}$, starting with $k=2$, by the time derivative in continuous time. Most generally, we thus have an expansion [9]

$$x_{kn}=\sum_{q=0}^{K-k}x_{(q+k)(n-N+1-p)}\frac{\tau^q(N-1+p)^q}{q!} \tag{2}$$

such that $k=1$ gives us (1) and $x_{Kn}=x_{K(n-N+1-p)}$ holds true for $k=K$.

If we now suppose that x_{1n} is measured as s_n in the presence of noise v_n having zero mean, $E\{v_n\}=0$, and arbitrary distribution and covariance $\mathbf{Q}(i,j)=E\{v_iv_j\}$ for all i and j, then the signal and measurement can be represented in state space, using (2), with the state and observation equations as, respectively,

$$\mathbf{x}_n=\mathbf{A}^{N-1+p}\mathbf{x}_{n-N+1-p}\,, \tag{3}$$

$$s_n=\mathbf{C}\mathbf{x}_n+v_n\,, \tag{4}$$

where the $K\times1$ state vector is given by

$$\mathbf{x}_n=[x_{1n}\,x_{2n}\,\ldots\,x_{Kn}]^T\,. \tag{5}$$

The $K\times K$ triangular matrix $\mathbf{A}$ is specified as

$$\mathbf{A}=\begin{bmatrix}1 & \tau & \frac{\tau^2}{2} & \ldots & \frac{\tau^{K-1}}{(K-1)!}\\ 0 & 1 & \tau & \ldots & \frac{\tau^{K-2}}{(K-2)!}\\ 0 & 0 & 1 & \ldots & \frac{\tau^{K-3}}{(K-3)!}\\ \vdots & \vdots & \vdots & \ddots & \vdots\\ 0 & 0 & 0 & \ldots & 1\end{bmatrix}, \tag{6}$$

the power $\mathbf{A}^i$ projects the state from $n-N+1-p$ to n, and the $1\times K$ measurement matrix is

$$\mathbf{C}=[\,1\quad 0\quad \ldots\quad 0\,]\,. \tag{7}$$

Employing (3) and (4), smoothing of the model state can now be organized as in the following.

3. UNBIASED SMOOTHING FIR FILTER

Smoothing FIR filtering of x_{1n} can be provided if to represent (3) and (4) on an interval of N points from $n-N+1-p$ to $n+p$, $p<0$, using recursively computed forward-in-time solutions [16] as

$$\mathbf{X}_N(p) = \mathbf{A}_N \mathbf{x}_{n-N+1-p}\,, \tag{8}$$

$$\mathbf{S}_N(p) = \mathbf{C}_N \mathbf{x}_{n-N+1-p} + \mathbf{U}_N(p)\,, \tag{9}$$

where

$$\mathbf{X}_N(p) = \left[\mathbf{x}_{n-p}^T \mathbf{x}_{n-1-p}^T \dots \mathbf{x}_{n-N+1-p}^T\right]^T, \tag{10}$$

$$\mathbf{S}_N(p) = \left[s_{n-p}\, s_{n-1-p} \dots s_{n-N+1-p}\right]^T, \tag{11}$$

$$\mathbf{U}_N(p) = \left[v_{n-p}\, v_{n-1-p} \dots v_{n-N+1-p}\right]^T, \tag{12}$$

$$\mathbf{A}_N = \left[\ (\mathbf{A}^{N-1+p})^T \quad \dots \quad (\mathbf{A}^{1+p})^T \quad (\mathbf{A}^p)^T\ \right]^T, \tag{13}$$

$$\mathbf{C}_N = \begin{bmatrix} \mathbf{C}\mathbf{A}^{N-1+p} \\ \vdots \\ \mathbf{C}\mathbf{A}^{1+p} \\ \mathbf{C}\mathbf{A}^{p} \end{bmatrix} = \begin{bmatrix} (\mathbf{A}^{N-1+p})_1 \\ \vdots \\ (\mathbf{A}^{1+p})_1 \\ (\mathbf{A}^{p})_1 \end{bmatrix}, \tag{14}$$

where $(\mathbf{Z})_1$ means the first row of a matrix $\mathbf{Z}$.

Given (8) and (9), the smoothing FIR filtering estimate of x_{1n} can be obtained as follows:

$$\begin{aligned} \hat{x}_{1n|n-p} &= \sum_{i=p}^{N-1+p} h_{li}(p) s_{n-i} && \text{(15a)} \\ &= \mathbf{W}_l^T(p)\mathbf{S}_N && \text{(15b)} \\ &= \mathbf{W}_l^T(p)[\mathbf{C}_N \mathbf{x}_{n-N+1-p} + \mathbf{U}_N(p)]\,, && \text{(15c)} \end{aligned}$$

where $h_{li}(p) \triangleq h_{li}(N,p)$ is the l-degree FIR filter gain [15] dependent on N and p [9,10] and the l-degree and $1 \times N$ filter gain matrix is given by

$$\mathbf{W}_l^T(p) = \left[h_{lp}(p)\, h_{l(1+p)}(p) \dots h_{l(N-1+p)}(p)\right] \tag{16}$$

that is to be specified in the minimum bias sense.

3.1 Unbiased Polynomial Gain

The unbiased smoothing FIR filtering estimate can be found if we start with the unbiasedness condition

$$E\{\hat{x}_{1n|n-p}\} = E\{x_{1n}\}\,. \tag{17}$$

Combining $E\{x_{1n}\} = (\mathbf{A}^{N-1+p})_1 \mathbf{x}_{n-N+1-p}$ with the mean estimate $E\{\hat{x}_{1n|n-p}\} = \mathbf{W}_l^T(p)\mathbf{C}_N \mathbf{x}_{n-N+1-p}$ taken from (15c) leads to the unbiasedness constraint

$$(\mathbf{A}^{N-1+p})_1 = \bar{\mathbf{W}}_l^T(p)\mathbf{C}_N\,, \tag{18}$$

where $\bar{\mathbf{W}}_l(p)$ means the l-degree unbiased gain matrix.

It has been shown in [9] that (18) can alternatively be represented as

$$\bar{\mathbf{W}}_l^T(p)\mathbf{V}(p) = \mathbf{J}^T\,, \tag{19}$$

where $\mathbf{J} = [\underbrace{1\ 0\ \dots 0}_{N}]^T$ and the p-dependent and $N \times (l+1)$ Vandermonde matrix [17] is specified by

$$\mathbf{V}(p) = \begin{bmatrix} 1 & p & p^2 \\ 1 & 1+p & (1+p)^2 \\ 1 & 2+p & (2+p)^2 \\ \vdots & \vdots & \vdots \\ 1 & N-1+p & (N-1+p)^2 \end{bmatrix}. \tag{20}$$

Because the inverse of $\mathbf{V}^T(p)\mathbf{V}(p)$ exists, a solution to (19) can be written as

$$\bar{\mathbf{W}}_l^T(p) = \mathbf{J}^T[\mathbf{V}^T(p)\mathbf{V}(p)]^{-1}\mathbf{V}^T(p)\,. \tag{21}$$

Following [18], the component of (16) can further be represented with the degree polynomial

$$h_{li}(p) = \sum_{j=0}^{l} a_{jl}(p) i^j\,, \tag{22}$$

where $l \in [1,K]$, $i \in [p, N-1+p]$, and $a_{jl}(p) \triangleq a_{jl}(N,p)$ are still unknown coefficients.

Substituting (22) to (19) and rearranging the terms lead to a set of linear equations, having a compact matrix form of

$$\mathbf{J} = \mathbf{D}(p)\boldsymbol{\Upsilon}(p)\,, \tag{23}$$

where $\mathbf{J} = [\underbrace{1\ 0\ \dots 0}_{K}]^T$,

$$\boldsymbol{\Upsilon} = [\underbrace{a_{0(K-1)}\ a_{1(K-1)}\ \dots a_{(K-1)(K-1)}}_{K}]^T, \tag{24}$$

and a low dimensional, $l \times l$, symmetric matrix $\mathbf{D}(p)$ is specified via (20) as

$$\begin{aligned} \mathbf{D}(p) &= \mathbf{V}^T(p)\mathbf{V}(p) \\ &= \begin{bmatrix} d_0(p) & d_1(p) & \dots & d_l(p) \\ d_1(p) & d_2(p) & \dots & d_{l+1}(p) \\ \vdots & \vdots & \ddots & \vdots \\ d_l(p) & d_{l+1}(p) & \dots & d_{2l}(p) \end{bmatrix}. \end{aligned} \tag{25}$$

The component in (25) can be developed as in [10],

$$\begin{aligned} d_m(p) &= \sum_{i=p}^{N-1+p} i^m\,, \quad m = 0,1,\dots 2l\,, && (26) \\ &= \frac{1}{m+1}\left[B_{m+1}(N+p) - B_{m+1}(p)\right], && (27) \end{aligned}$$

where $B_n(x)$ is the Bernoulli polynomial.

An analytic solution to (23) gives us the coefficient

$$a_{jl}(p) = (-1)^j \frac{M_{(j+1)1}(p)}{|\mathbf{D}(p)|}\,, \tag{28}$$

where $|\mathbf{D}|$ is the determinant of $\mathbf{D}(p)$, turning out to be p-invariant, and $M_{(j+1)1}(p)$ is the minor of $\mathbf{D}(p)$.

3.2 p-Lag Polynomial Ramp Unbiased Gain

It can now be shown that the 1-degree p-shift polynomial ramp unbiased gain existing from p to $N-1+p$ is specified, by (22) and (28), as

$$h_{1i}(p) = a_{01}(p) + a_{11}(p)i\,, \tag{29}$$

with the coefficients

$$a_{01}(p) = \frac{2(2N-1)(N-1)+12p(N-1+p)}{N(N^2-1)}\,, \tag{30}$$

$$a_{11}(p) = -\frac{6(N-1+2p)}{N(N^2-1)}\,. \tag{31}$$

In turn, the noise power gain (NPG) associated with (29) is provided to be [4]

$$\begin{aligned} g_1(p) &= a_{10}(p) \\ &= \frac{2(2N-1)(N-1)+12p(N-1+p)}{N(N^2-1)}\,. \end{aligned} \tag{32}$$

We notice that, by $p=0$, the gain (29) becomes that originally derived in [19] via linear regression and rederived in [15] in state space. This gain was further modified to be optimal in the minimum MSE sense in [20] and, in [4], one can find the higher degree gains along with the relevant NPG analysis.

4. APPLICATIONS

Below we apply the solutions discussed to the problems associated with smoothing and prediction of time errors in the local and master clocks.

4.1 The Best Linear Fit for a Two-State Clock Model

To demonstrate efficiency of (29), below we find the best linear unbiased fit for the crystal clock time interval error (TIE) [15]. Before doing so, we notice that linear prediction is stated in [6, 8, 21] to be optimum or near optimum for the prediction of clock instabilities [22]. Therefore, (29) would certainly provide the best extrapolation of errors.

The TIE of a crystal clock imbedded in the Stanford Frequency Counter SR620 was measured each second during 357332 s using another SR620 for the reference cesium clock (Symmetricom CsIII) as shown in Fig. 1 as "x_n+ noise". On the interval of $N = 357333$ points, the clock was identified to have two states. For the two-state model, the ramp FIR smoother was organized by changing a variable in (15a) and (29) to produce the estimate at $n+p$ as

$$\tilde{x}_{1(n+p)|n} = \sum_{i=0}^{N-1} \tilde{h}_{1i}(N,p)s_{n-i}\,, \tag{33}$$

where

$$\tilde{h}_{1i}(N,p) = \frac{2(2N-1)-6i}{N(N+1)} + \frac{6p(N-1-2i)}{N(N^2-1)}\,. \tag{34}$$

To find the best fit, all the data must be involved. We thus substitute N with $n+1$ and modify (33) to

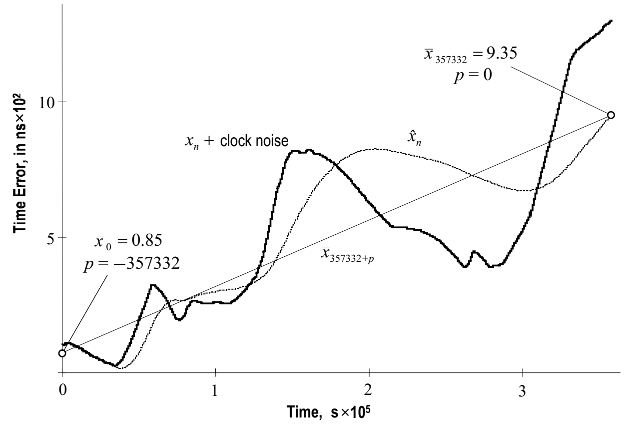

Figure 1: Unbiased FIR filtering and smoothing of the crystal clock TIE.

$$\tilde{x}_{n+p} = \sum_{i=0}^{n} \tilde{h}_{1i}(n+1,p)s_{n-i}\,, \tag{35}$$

where

$$\tilde{h}_{1i}(n+1,p) = \frac{2n(2n+1)-6in+6p(n-2i)}{n(n+1)(n+2)}\,. \tag{36}$$

The best linear fit appears if to smooth the data at the initial point with $p=-n$ as $\tilde{x}_0$ and filter at the current point with $p=0$ as $\hat{x}_n$. A straight line $\bar{x}_n$ passing through two these points is provided with

$$\begin{aligned} \bar{x}_{n+p} &= \tilde{x}_0 + (n+p)\frac{\hat{x}_n - \tilde{x}_0}{n} && \text{(37a)} \\ &= \sum_{i=0}^{n} \tilde{h}_{1i}(n+1,p)s_{n-i} && \text{(37b)} \end{aligned}$$

if we fix n and change p from $-n$ to 0, as a variable for $\tilde{h}_{1i}(n+1,p)$ given with (36).

An evolution of the last point of the best fit provided by the filtering estimate with $p=0$ at n is represented in Fig. 1 with $\hat{x}_n$. This estimate is obtained by (35) with n changed from 0 to $n = 357332$. As can be observed, $\hat{x}_n$ unbiasedly tracks the mean of the "x_n+ clock noise".

The best fit is shown in Fig. 1 for all the measured points as a straight line $\bar{x}_{357332+p}$ having the values of $\bar{x}_0 = 0.85$ ns with $p=-357332$ and $\bar{x}_{357332} = 9.35$ ns with $p=0$. Similarly, it an be provided employing the higher degree gains. In each of the cases, the fit will hold true only for the observed database. It would be corrected for every new measurement point added to the data.

4.2 An Application to the USNO Master Clock

The USNO has published on the WEB site the UTC – UTC(USNO MC) time differences (73 points) measured each 5 days in 2008, as issued monthly by BIPM [units are in Modified Julian Dates (MJDs) and nanoseconds]. For this measurement, we form the time scale starting with $n=0$ (54464.0 MJD) and finishing at $n=72$ (54829.0 MJD). The measurement is shown in Fig. 1a (circles).

Because the frequency drift in the USNO MC is negligibly small and measurement is provided with negligible errors, the clock can be represented with the two-state space model, $K = 2$,

$$\mathbf{x}_n = \mathbf{A}\mathbf{x}_{n-1} + \mathbf{w}_n \,, \quad (38)$$

$$s_n = \mathbf{C}\mathbf{x}_n \,, \quad (39)$$

in which

$$\mathbf{x}_n = \begin{bmatrix} x_n \\ y_n \end{bmatrix}, \quad \mathbf{A} = \begin{bmatrix} 1 & \tau \\ 0 & 1 \end{bmatrix}, \quad \mathbf{C} = [1\,0] .$$

The time scale of the USNO MC is corrected. Therefore, the time error noise can be considered to be zero-mean and white. We calculate the variance of this noise as $\sigma_{xn}^2 = E\{w_n^2\}$ providing the averaging from zero to the current point n. The second clock state can be represented by the time derivative of the first state and the noise variance calculated similarly. Accordingly, we form the clock noise vector as $\mathbf{w}_n = [w_{xn}\ w_{yn}]^T$ and the covariance matrix with

$$\mathbf{\Psi}_n = \begin{bmatrix} \sigma_{xn}^2 & E\{w_{xn}w_{ym}\} \\ E\{w_{yn}w_{xm}\} & \sigma_{yn}^2 \end{bmatrix},$$

where $0 \leqslant m \leqslant n$. Note that the effect of frequency noise is relatively small in $\mathbf{\Psi}_n$.

Figure 2 sketches the estimates of the clock first state x_n and second state y_n provided by the optimal estimator [24] and unbiased one (15a) with $p \lesseqgtr 0$. Estimates of the first state are illustrated in Fig. 2a. This figure reveal that the optimal and unbiased estimates differ in average on about 15% and that this measure can reach 50% at some points. Although a comparison of optimal and unbiased estimates is a special topic, there is an immediate explanation to differences with small N. The unbiased filter provides the best fit for the noisy process, whereas in the optimal filter this fit is adjusted by the noise covariance function. On the one hand, the latter cannot be ascertained correctly with a small number of measurements. Therefore, the optimal filter may produce errors. On the other hand, the unbiased filter is associated with large horizons and may not be precise otherwise. So, we have an inconsistency that would be reduces by increasing N.

Smoothing with $p < 0$ and prediction with $p > 0$ of time errors is illustrated in Fig. 2b. Here, we also employ the p-shift optimal algorithm [24] and the p-shift unbiased estimate (15a). For the illustrative purposes, we fix three time points, $n = 21$, $n = 36$, and $n = 56$, and allow negative p to provide smoothing and positive p to obtain prediction. Smoothing and prediction lines are depicted in Fig. 2b with the right and left arrows, respectively. It can be shown that the unbiased prediction is exactly that found in [22] employing the ramp FIR filter. In [22], one can also find an unbiased prediction of clock errors [23] obtained with a 5-point step and unbiased smoothing of measurement providing the best fit. An important observation can be made observing Fig. 2b. It is seen that the unbiased smoothing function ranging from $n = 36$ to zero fits better than the optimal one. However, this fact does not mean that the optimal smooth is lesser accurate, because the latter fits better the full measurement.

Finally, Fig. 2c sketches filtering estimates of the second clock state provided with the optimal and unbiased filters.

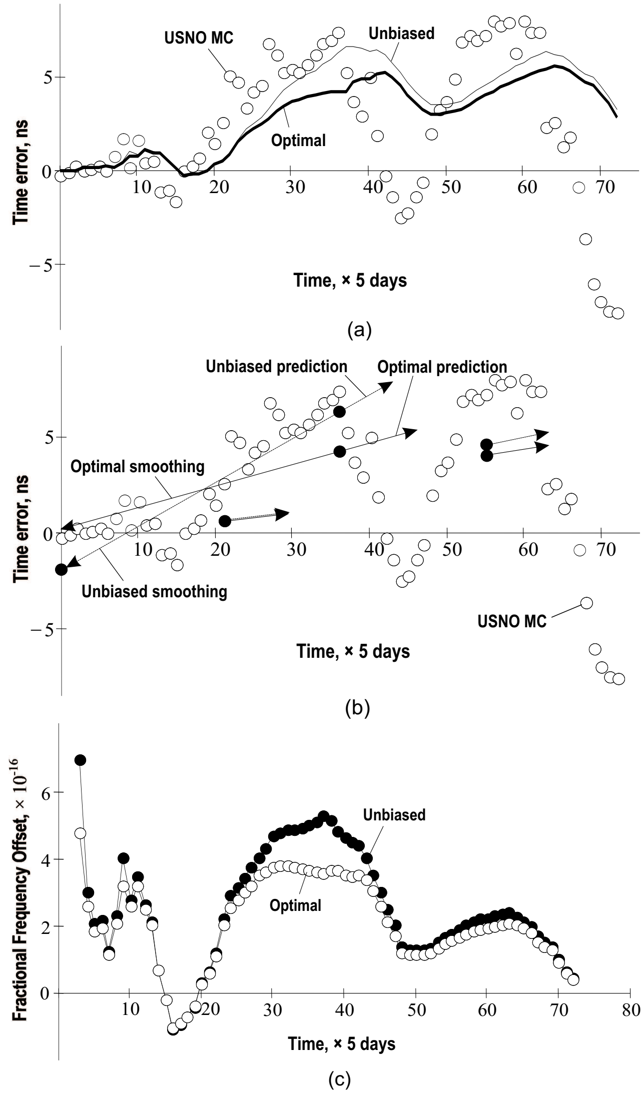

Figure 2: FIR estimates of the USNO MC current state via the TIE measured during 2008 each 5 days: (a) filtering of the first state x_n, (b) prediction and smoothing of the first state, and (c) filtering of the second state y_n.

Again we infer that both estimates are consistent, except for the region from $n = 25$ to $n = 45$, in which the discrepancy reaches 50%.

5. CONCLUSIONS

In this paper, we discussed unbiased smoothing FIR filtering of discrete-time polynomial signals represented in state space. The relevant gain for the FIR structure was found in the matrix form with no requirements for noise and initial conditions. This gain was also developed in the unique polynomial form having strong engineering features. The unbiased ramp gain was applied practically to the crystal clock TIE. A high efficiency of the proposed solution is demonstrated graphically. We finally notice that, even visually, the best linear fit demonstrated in Fig. 1 provides us with the best extrapolation (prediction) of future clock behaviors that is required by the IEEE Standard 1139 [6] and can be used in the holdover mode in digital communications and other networks. Estimation with $p < 0$ turned out to be useful to smooth time errors and fractional frequency offsets in master clocks as well.

REFERENCES

[1] A. Savitzky and M. J. E. Golay, “Smoothing and differentiation of data by simplified least square procedure,” *Analytical Chemistry*, vol. 36, pp. 1627–1639, July 1964.

[2] T. Kailath, “A view of three decades of linear filtering theory,” *IEEE Tram. Inform. Theory*, vol. IT-20, pp. 145–181, March 1974.

[3] A. V. Oppenheim and R. W. Schafer, *Discrete Time Signal Processing*, Upper Saddle River, NJ: Prentice-Hall, 1998.

[4] Y. S. Shmaliy and L. J. Morales-Mendoza “FIR smoothing of discrete-time polynomial signals in state space,” *IEEE Trans. on Signal Process.*, vol. 58, pp. 862–870, May 2006.

[5] L. J. Morales-Mendoza and Y. S. Shmaliy, “Moving average hybrid filter to the enhancinbg ultrasonic image processing,” *IEEE Latin America Trans.*, vol. 8, pp. 9–15, March 2010.

[6] *IEEE Standard Definitions of Physical Quantities for Fundamental Frequency and Time Metrology – Random Instabilities*, IEEE Standard 1139-1999; IEEE: Piscataway, NJ, 1999, pp. 1-36.

[7] ITU-T Recommendation G.811: Timing characteristics of primary reference clocks, 1997.

[8] A Lepek, “Clock prediction and characterization,” *Metrologia*, vol. 34, no. 5, pp. 379-386, Oct. 1997.

[9] Y. S. Shmaliy, “An unbiased *p*-step predictive FIR filter for a class of noise-free discrete-time models with independently observed states,” *Signal, Image and Video Process.*, vol. 3, no. 2, pp. 127–135, Jun. 2009.

[10] Y. S. Shmaliy and L. Arceo-Miquel, “Efficient predictive estimator for holdover in GPS-based clock synchronization,” *IEEE Trans. on Ultrason., Ferroel. and Freq. Contr.*, vol. 55, no. 10, pp. 2131–2139, Oct. 2008.

[11] C. K. Ahn and P. S. Kim, “Fixed-lag maximum likelihood FIR smoother for state-space models,” *IEICE Electronics Express*, vol. 5, pp. 11–16, 2008.

[12] J. H. Kim and J. Lyou, “Target state estimation design using FIR filter and smoother,” *Trans. on Control, Automation and System Engineering*, vol. 4, pp. 305–310, December 2002.

[13] Y. S. Shmaliy, “Optimal gains of FIR estimators for a class of discrete-time state-space models,” *IEEE Signal Process. Letters*, vol. 15, pp. 517–520, 2008.

[14] Y. S. Shmaliy and O. Ibarra-Manzano, “Optimal FIR filtering of the clock time errors,” *Metrologia*, vol. 45, no. 5, pp. 571–576, Sep. 2008.

[15] Y. S. Shmaliy, “An unbiased FIR filter for TIE model of a local clock in applications to GPS-based timekeeping,” *IEEE Trans. on Ultrason., Ferroel. and Freq. Contr.*, vol. 53, no. 5, pp. 862–870, May 2006.

[16] H. Stark and J. W. Woods, *Probability, Random Processes, and Estimation Theory for Engineers*, 2^{nd} Ed., Prentice Hall, Upper Saddle River, NJ, 1994.

[17] R. A. Horn and C. R. Johnson, *Topics in Matrix Analysis*, New York: Cambridge Univ. Press, 1991.

[18] Y. S. Shmaliy, “Unbiased FIR filtering of discrete-time polynomial state-space models,” *IEEE Trans. Signal Process.*, vol. 57, no. 4, pp. 1241–1249, Apr. 2009.

[19] Y. S. Shmaliy, “A simple optimally unbiased MA filter for timekeeping,” *IEEE Trans. on Ultrason., Ferroel. and Freq. Control*, vol. 49, no. 6, pp. 789–797, Jun. 2002.

[20] Y. S. Shmaliy, “On real-time optimal FIR estimation of linear TIE models of local clocks,” *IEEE Trans. on Ultrason., Ferroel. and Freq. Contr.*, vol. 54, no. 11, pp. 2403–2406, Nov. 2007.

[21] G. Busca, Q. Wang, “Time prediction accuracy for space clocks,” *Metrologia*, vol. 40, no. 3, pp. S265–S269, Jun. 2003.

[22] Y. S. Shmaliy, “Linear unbiased prediction of clock errors,” *IEEE Trans. on Ultrason., Ferroel. and Freq. Contr.*, vol. 56, no. 9, pp. 2027–2029, Sep. 2009.

[23] F. Vernotte, J. Delporte, M. Brunet, T. Tournier, “Uncertainties of drift coefficients and extrapolation errors: Applications to clock error prediction,” *Metrologia*, vol. 38, no. 4, pp. 325–342, Aug. 2001.

[24] Y. S. Shmaliy, “Linear optimal estimation of discrete time-invariant state-space models,” *IEEE Trans. on Signal Process.*, vol. 58, no. 6, pp. 3086–3096, Jun. 2010.